International Journal of Research in Engineering and Science (IJRES)
ISSN (Online): 2320-9364, ISSN (Print): 2320-9356
www.ijres.org Volume 2 Issue 11 ǁ November. 2014 ǁ PP.38-50

Thermodynamic characterization of metal dissolution and inhibitor adsorption processes on mild steel by 1-hexyl-3-methylimidazolium chloride in 2M sulphuric acid medium

S. Velrani[1], B. Jeyaprabha[2], P. Prakash[3*]
[1]Department of Chemistry, Karpagam University, Coimbatore, Tamilnadu, India
[2]Department of Civil Engineering, Fatima Michael College of Engineering & Technology, Madurai, India
[3*]Department of Chemistry, Thiagarajar College, Madurai, Tamilnadu, India

ABSTRACT : *The inhibition effect of 1-hexyl-3-methylimidazolium chloride (HMIC) on the corrosion of mild steel in 2M sulphuric acid solution has been investigated by weight loss. potentiodynamic polarization and electrochemical impedance spectroscopy. The effect of temperature on the corrosion behavior of mild steel in 2M H_2SO_4 with addition of inhibitor was studied in weight loss method at the temperature range of 308-328 K. Results obtained that the inhibition efficiency increases with increasing the concentration of the inhibitor and decreases with increasing the temperature. Polarization and impedance measurements were in good agreement. The adsorption of this inhibitor on the mild steel surface obeys the Langmuir adsorption isotherm. Fourier transform spectroscopy (FTIR) and Scanning electron microscopy (SEM) was also carried out to establish the corrosion inhibit property of this inhibitor in sulphuric acid medium. Quantum chemical calculations were performed using density functional theory to find out whether a clear link exists between the inhibitive effect of the inhibitor and the electronic properties of its main constituents.*

Key words: *Inhibitor, Mild steel, Thermodynamics, Impedance, Polarization*

I. INTRODUCTION

The use of inhibitors is one of the most practical methods for protection against corrosion, especially in acidic solution. The organic compounds are widely used as acid inhibitors in industrial operations, such as pickling, cleaning, acidification of oil wells, to protect metals and alloys [1]. During the past decade, the inhibition of mild steel in acid solutions by different types of organic inhibitor has been extensively studied [2-6]. The organic substances mainly contain hetero atoms as sulfur, phosphorus, nitrogen, oxygen atoms, and multiple bonds in the molecules that facilitate the adsorption on the metal surface are strongly polar [7-8]. The polar unit is regarded as the reaction centre for the adsorption process. Thus, polar organic compounds are adsorbed on the metal surface, forming a charge transfer complex bond between their polar atoms and the metal. The size, shape and electronic charge on the molecule determine the degree of adsorption and hence the effectiveness of the inhibitor [9-10].

In this study, the inhibition potential of 1-hexyl-3-methylimidazolium chloride in 2M H_2SO_4 through weight loss, electrochemical impedance spectroscopy, potentiodynamic polarization studies, Fourier transform infrared spectroscopy (FTIR), Scanning electron microscopy (SEM) and Quantum chemical calculation have been investigated.

II. EXPERIMENTAL

The corrosion tests were performed in 2M H_2SO_4 solution in the absence and presence of HMIC. The inhibitor (HMIC) was purchased from Sigma Aldrich Company. The chemical structure of HMIC is shown in Fig.1. The corrosive solution of 2M H_2SO_4 (AR grade) was prepared in distilled water and used for all studies. The concentrations of the inhibitor employed were varied from 0.002M to 0.01M in acid medium. For each experiment, a freshly prepared solution was used.

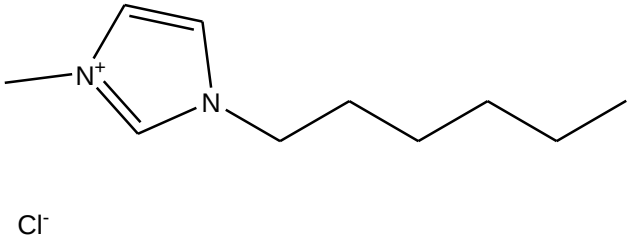

Figure 1: Chemical structure of HMIC.

The mild steel specimens of 3cmx3cmx0.6cm dimensions were abraded with different grades of emery papers, washed with distilled water, degreased with acetone, dried with air. After weighing accurately the specimens were immersed in solutions containing 2M H_2SO_4 solution with and without various concentrations of HMIC. The experimental studies were performed at different temperature (from 308K to 328K) maintained in a thermostated water bath. The temperature maintenance in all immersion was around 24 hrs. The solution volume was 100 ml. The coupons were withdrawn from the tested solution, washed thoroughly with distilled water followed by acetone and dried with air, then weighed again. Weight loss was used to calculate the corrosion rate (ρ) and inhibition efficiency (IE) as follows:

$$\rho = W_b\text{-}W_a / St \quad (1)$$

where W_b and W_a are the specimen weight before and after immersion in the test solution respectively, S is the surface area of the specimen and t is the end time of each experiment. The IE (%) values were being calculated from weight loss data by using Eq. (2):

$$IE(\%) = [\rho^{\circ}\text{-}\rho/\rho^{\circ}]\times 100 \quad (2)$$

where ρ° is a corrosion rate without inhibitor and ρ is a corrosion rate with inhibitor.

Polarization study was carried out using H & CH electrochemical workstation impedance Analyzer Model CHI 604D provided with iR compensation facility, using three-electrode cell assembly. A double wall one-compartment cell with a three-electrode configuration was used. Mild steel was used as a working electrode and platinum electrode as counter electrode and calomel as reference electrodes. After having done iR compensation, polarization study was carried out at sweep rate 0.005V/sec. The corrosion parameters such as linear polarization (LPR), Corrosion potential (E_{corr}), corrosion current (I_{corr}) and Tafel slopes (b_c and b_a) were measured. During the polarization study, the scan rate (v/s) was 0.005; Hold time at Ef (s) was zero and quiet time (s) was 2. AC impedance spectra were recorded in the same instrument using three-electrode cell assembly. The real part and imaginary part of the cell impedance were measured in ohms for various frequencies. The charge transfer resistance (R_{ct}) and double layer capacitance (C_{dl}) values were calculated using the relation:

$$R_{ct} = (R_s + R_{ct}) - R_s \quad (3)$$
$$C_{dl} = ½\pi R ctf_{max} \quad (4)$$

Where f_{max} = maximum frequency and R_s = Solution resistance. AC impedance was recorded with initial E(v) = 0 High frequency (Hz) = 1×105, Low frequency (Hz) = 0.1, Amplitude (v) = 0.005 and Quiet time (s) = 2. The working surface area was 0.5cm^2, abraded with emery paper (grade 600-1200) on test face, rinsed with distilled water, degreased with acetone, and dried with a cold air steam. Before measurement the electrode was immersed in test solution at open circuit potential (OCP) for 10 min to be sufficient to attain a stable state. All electrochemical measurements were carried out at 308K using 50ml of electrolyte (2M H_2SO_4) in stationary condition. Each experiment was repeated at least three times to check the reproducibility.

The mild steel specimens were immersed in acid solutions in the presence and absence of inhibitor for a period of 24 h. After 24 h, the specimens were taken out and dried. The nature of the surface film formed on the surface of the mild steel specimen was analyzed by using JEOL (JSM 6390) Scanning electronic microscopy.

The HMIC (Coated on KBr disc) was characterized by FT-IR spectroscopy (8400S SHIMADZU spectrometer. After immersion in 2M H_2SO_4 with addition of HMIC for 24 h, the specimen was cleaned with distilled water, dried with a cold air. Then the thin adsorption layer formed on steel surface was rubbed and it was characterized by the same spectrophotometer.

III. RESULT AND DISCUSSION

3.1. Weight loss studies:

The values of corrosion rate and the percentage inhibition efficiency (%IE) obtained from weight loss measurements for mild steel at different concentration of HMIC in 2M H_2SO_4 at different temperatures is summarized in Table 1. The values of corrosion rate and the percentage inhibition efficiency (%IE) obtained from weight loss measurements for mild steel at different concentration of HMIC in 2M H_2SO_4 at different temperatures is summarized in Table 1.

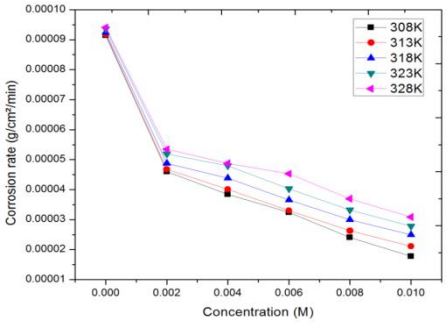

Figure 2: Effect of corrosion rate on the concentration of HMIC at different temperatures.

Table 1 Influence of temperature on the corrosion rate of mild steel in 2M H_2SO_4 at different concentrations of HMIC and the corresponding corrosion inhibition efficiency.

Temperature(K)	Concentration (M)	Corrosion Rate($x10^{-5}$)	Inhibition Efficiency (%)
308	Blank	9.14	-
	0.002	4.6	49.67
	0.004	3.84	57.99
	0.006	3.24	64.55
	0.008	2.41	73.63
	0.01	1.78	80.52
313	Blank	9.18	-
	0.002	4.68	49.02
	0.004	4.01	56.32
	0.006	3.3	64.05
	0.008	2.63	71.35
	0.01	2.11	77.02
318	Blank	9.24	-
	0.002	4.88	47.19
	0.004	4.38	52.60
	0.006	3.66	60.39
	0.008	3.0	67.53
	0.01	2.5	72.9
323	Blank	9.36	-
	0.002	5.19	44.55
	0.004	4.8	48.72
	0.006	4.03	56.94
	0.008	3.32	64.53
	0.01	2.78	70.30
328	Blank	9.41	-
	0.002	5.35	43.15
	0.004	4.88	48.14
	0.006	4.53	51.86
	0.008	3.7	60.68
	0.01	3.09	67.16

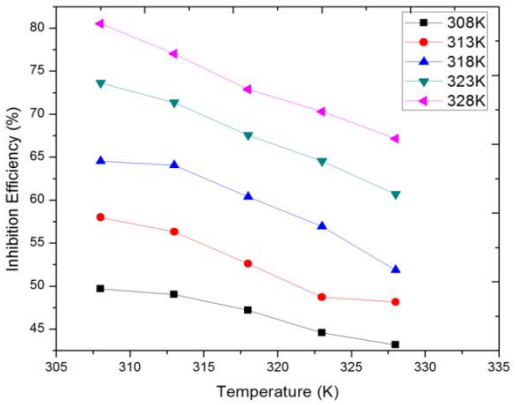

Figure 3: Variation of inhibition efficiency with different temperatures at different concentrations of HMIC.

Fig. 2 shows the Dependence of mild steel corrosion rate on the concentration of HMIC in acid medium at different temperatures and the Fig 3 shows the variation of the inhibition efficiency with inhibitor concentration of HMIC at different temperatures. It is noted that the corrosion rate decreases and the inhibition efficiency increases with increasing the concentration of HMIC with decreasing the temperature. It is clear that the inhibitor concentration increase the number of molecules adsorbed over the mild steel surface and blocks the active sites in which direct acid attack proceeds, and protects the metal from corrosion.

3.2. Potentiodynamic polarization studies:

Table 2 Potentiodynamic polarization parameters for the corrosion of mild steel in 2M H_2SO_4 in the absence and the presence of HMIC.

C_{inh} (M)	E_{corr} (mV)	i_{corr} (Acm^{-2})	b_c	b_a	R_p	%IE
Blank	-0.524	$6.039x10^{-3}$	4.876	7.125	6.0	-
0.002	-0.521	$4.867x10^{-3}$	5.256	7.386	7.1	19.41
0.004	-0.521	$2.729x10^{-3}$	5.030	8.560	11.7	54.81
0.006	-0.522	$2.598x10^{-3}$	5.107	8.760	12.1	56.98
0.008	-0.525	$1.594x10^{-3}$	5.171	9.542	18.5	73.61
0.01	-0.526	$1.429x10^{-3}$	5.097	9.953	20.2	76.34

The potentiodynamic polarization curves of mild steel in absence and presence of various concentrations of the HMIC in 2M H_2SO_4 are shown in Fig 4 and various electrochemical parameters such as corrosion potential (E_{corr}), corrosion current density (I_{corr}), percentage inhibition efficiency (%IE) and Tafel constants (b_a and b_c) obtained from cathodic and anodic curves are given in Table 2.

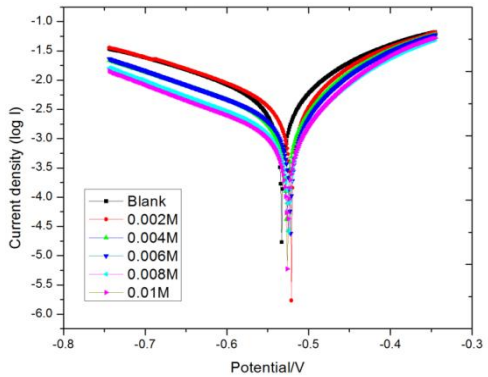

Figure 4: Tafel plots for mild steel immersed in 2M H_2SO_4 containing different concentration of HMIC at 308K.

The inhibition efficiency was calculated from polarization measurements according to the relation given below;

$$IE\% = (i^0_{corr} - i_{corr} / i^0_{corr}) \times 100 \quad (5)$$

where i^0_{corr} and i_{corr} are the uninhibited and inhibited corrosion current densities, respectively.

It is observed that the inhibitor suppressed the cathodic reaction to greater extent than the anodic one at all the concentrations. In other words, inhibitor under investigation predominantly inhibits cathodic and anodic corrosion.

3.3. Electrochemical impedance spectra studies:

Electrochemical impedance spectra for mild steel in 2M H_2SO_4 interface in absence and presence of HMIC were represented in Table 3 and Fig 5. The Nyquist plots contain depressed semicircle with the center under the real axis, whole size increases with the inhibitor indicating a charge transfer process mainly controlling the corrosion of mild steel. Such a behavior characteristics for solid electrodes and often referred to as frequency dispersion that has been attributed to roughness and other in homogeneities of solid surface.

Table 3 Electrochemical impedance parameters for mild steel in 2M H_2SO_4 in the absence and the presence of HMIC.

C_{inh} (M)	R_s (□ cm^2)	R_{ct} (□ cm^2)	C_{dl} (F/cm^2)	%IE
Blank	1.639	2.111	11.82x10^{-2}	-
0.0002	1.693	3.856	3.636x10^{-2}	45.25
0.0004	1.627	4.314	2.795x10^{-2}	51.07
0.0006	1.531	8.759	0.740x10^{-2}	75.90
0.0008	1.595	9.445	0.624x10^{-2}	77.65
0.001	1.656	13.38	0.315x10^{-2}	84.23

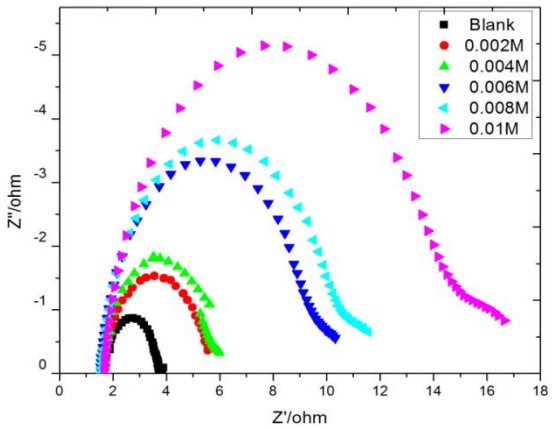

Figure 5: Nyquist plots for mild steel immersed in 2M H_2SO_4 containing different concentration of HMIC at 308K.

It is apparent from these plots that the impedance response of mild steel in uninhibited acid solution has significantly changed after the addition of the inhibitor in the corrosion solutions. This indicated that the impedance of the inhibited substrate has increased with increasing concentration of HMIC. The values of charge transfer resistance (R_{ct}) and double layer capacitance (C_{dl}) are obtained from Nyquist plot. The inhibition efficiency was calculated using the following equation:

$$IE\% = (R^1_{ct} - R_{ct} / R^1_{ct}) \times 100 \quad (6)$$

where R^1_{ct} and R_{ct} are the values of the charge transfer resistance observed in the absence and presence of inhibitor molecules. The R_{ct} values increased with the increasing concentration of the inhibitor. On the other hand, the value of C_{dl} decreased with an increase in inhibitor concentration. This situation was the result of increasing the surface coverage by the inhibitor, which lead to an increase in the inhibition efficiency.

3.4. Adsorption isotherms:

The degrees of surface coverage (θ) for different inhibitor concentrations were evaluated by weight loss data. Data were tested graphically fitting to various isotherms. The following adsorption isotherms are the most common models to study the mechanism of corrosion inhibition [11-14].

Freunlich isotherm: $\log \theta = \log K_{ads} + n \log C$ (7)

Langmuir isotherm: $\theta = K_{ads} C$ (8)

El-Awady isotherm: $\log \theta/1-\theta = \log K_{ads} + y \log C$ (9)

Tempkin isotherm: $\exp(-2a\theta) = K_{ads} C$ (10)

where C is the inhibitor concentration. θ is the degree of the coverage on the metal surface and K_{ads} and n are the equilibrium constants for the adsorption-desorption process.

Table 4 Thermodynamic data for studied HMIC from experimental Langmuir adsorption isotherm

Temperature (K)	K_{ads}	ΔG_{ads} (kJ/mol)	Slope	R^2
308	3.066	-13.156	0.7030	0.994
313	2.772	-13.106	0.7173	0.996
318	2.854	-13.394	0.7033	0.985
323	2.570	-13.323	0.7107	0.986
328	2.180	-13.081	0.7328	0.984

Table 5 Thermodynamic data for studied HMIC from experimental Freunlich adsorption isotherm

Temperature (K)	K_{ads}	ΔG_{ads} (kJ/mol)	Slope	R^2
308	0.3262	-7.418	0.297	0.974
313	0.3608	-7.800	0.282	0.980
318	0.3980	-8.184	0.274	0.962
323	0.3890	-8.252	0.289	0.940
328	0.4587	-8.829	0.267	0.916

The experimental data fit best for Langmuir and Freunlich adsorption isotherms in acid medium. An inhibitor is found to obey Langmuir if plots of log C/θ Vs log C is linear. Similarly for Freunlich plot of log θ Vs log C will be linear in 2M H_2SO_4 medium. From the values of surface coverage, the linear regressions were calculated, and the parameters were listed in Table 4&5.

Fig. 6a is the relationship between C/θ and C in Langmuir adsorption isotherm and the Fig. 6b is the relationship between θ and C in Freunlich adsorption isotherm in acid medium. From that all the linear correlation coefficients (R^2) are nearly equal to 1, which indicates the adsorption of inhibitor onto steel surface obeys Langmuir and Freunlich adsorption isotherms.

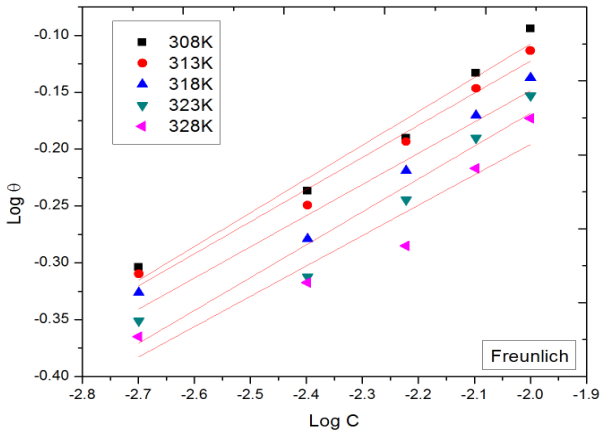

Figure 6a: Fitting Freunlich adsorption isotherm model for HMIC in 2M H_2SO_4 at different temperatures.

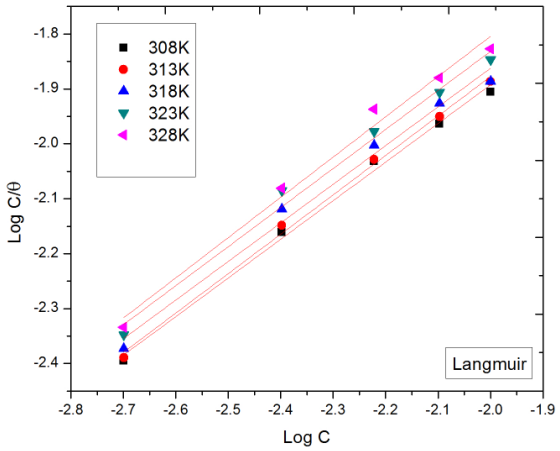

Figure 6b: Fitting Langmuir adsorption isotherm model for HMIC in 2M H_2SO_4 at different temperatures.

The most important thermodynamic adsorption parameters are free energy of adsorption (G_{ads}). The adsorption constant, K, is related to the standard free energy of adsorption, G_{ads} with the following equation [15].

$$G_{ads} = -RT\ln(55.5K_{ads}) \qquad (11)$$

where R is the gas constant, T is the temperature and 55.5 is the molar concentration of water in solution. The values of ΔG_{ads} were calculated from equation (11) and are recorded in Table 4&5**.** The negative values of G_{ads} indicate the stability adsorbed layer on the steel surface and spontaneity of the adsorption process. The dependence of G_{ads} on the temperature can be explained by two cases as follows:

(a) G_{ads} may increase (becomes less negative) with the increase temperature which indicates the occurrence of exothermic process.

(b) G_{ads} may decrease (becomes more negatives) with increasing temperature indicating occurrence of endothermic process.

Results presented in the Table 4&5 indicate that the values of ΔG_{ads} are negative in all cases. The negative values signify a spontaneous adsorption of the inhibitor molecules via physical adsorption mechanism ($\Delta G_{ads} \leq$ -20kJ/mol). It is also seen that the values of ΔG_{ads} decreased with an increase in temperature, a phenomenon which indicates that the adsorption of the inhibitor on to mild surface was unfavourable with increasing experimental temperatures as a result of desorption of adsorbed inhibitor from the metal surface. Generally, values of $\Delta G_{ads} \leq$ -20kJ/mol (as obtained in this study) signify physisorption, and values more negative than -40kJ/mol signify chemisorption ,physisorption is consistent with electrostatic interaction between charged molecules and a charged metal while chemisorption is consistent with charge sharing or transfer from the inhibitor components to the metal surface to form a co-ordinate type of bond[16-17].

3.5. Corrosion Kinetic parameters

Arrhenius suggested the famous equation which evaluates the temperature dependence of the rate constant as follows :

$$\log \rho = \log A - E^*_{app.}/ 2.303RT \qquad (12)$$

Here, A is the frequency factor and $E^*_{app.}$ is the apparent activation energy, R is the gas constant (R=8.314 J $mol^{-1}K^{-}$) and T is absolute temperature. Eq. (12) predicts that a plot of log ρ vs. 1/T should be a straight line (Fig 7). The slope of the line is ($-E^*_{app.}$ / 2.303R) and the intercept of the line extrapolated (1/T=0) gives log A, from which the values of A and Ea are recorded in Table 6.

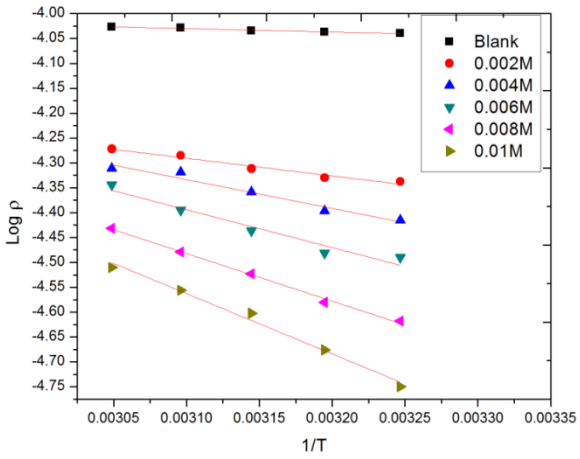

Figure 7: Arrhenius plots for log ρ vs 1/T for mild steel in 2M H_2SO_4 at different concentrations of HMIC.

Table 6 Activation parameters of the dissolution reaction of steel in 2M H_2SO_4in the absence and presence of HMIC.

Concentration (M)	E_a (kJ/ mol)	ΔH° (kJ/mol)	ΔS° (J/mol/K)
Blank	1.337	0.0832	-197.5544
0.002	6.982	0.1064	-197.5161
0.004	11.369	0.1213	-197.4587
0.006	17.351	0.1410	-197.5563
0.008	18.77	0.1478	-197.3821
0.01	23.723	0.1654	-197.3438

In general E^*_{app} values for the inhibited solutions (in the studied range of inhibitor concentration) are higher than that for the uninhibited one, indicating a strong inhibitive action for the studied compounds by increasing the energy barrier for the corrosion process, emphasizing the electrostatic character of the inhibitors adsorption on mild steel surface. $E^*_{app.}$ value for the inhibited system increases with inhibitor concentration in acid medium (Fig 8).

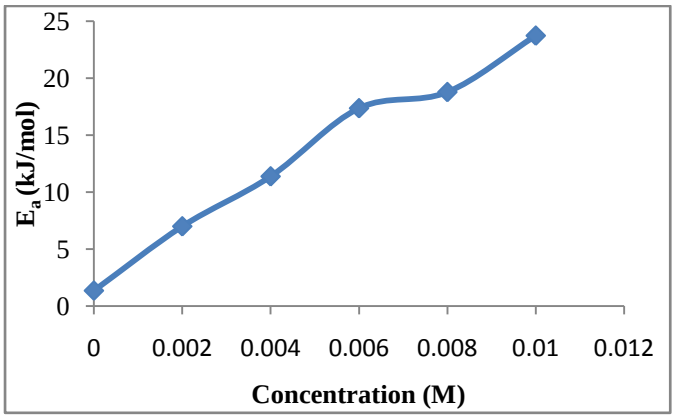

Figure 8: Dependence of apparent activation energy on the concentration of HMIC.

On the other hand, the change of enthalpy (ΔH°) and entropy (ΔS°) of activation for formation of the activation complex in the transition state can be obtained from the transition state equation:

$$\log \rho/T = [(\log(\frac{R}{hN})) + (\frac{\Delta S^{\circ}}{2.303R})] - \frac{\Delta H^{\circ}}{2.303RT} \quad (13)$$

where h is Plank's constant and N is the Avogadro's number. A plot of log ρ/T vs. 1/T gives straight line (Fig.9). The slope is (-ΔH˚/2.303R) and the intercept is [(log(R/ hN) + (ΔS˚ / 2.303R)], from which the values of ΔH˚ and ΔS˚ are calculated and recorded in Table 6.

The negative values for ΔS° in the inhibited and uninhibited system implies that the activation complex in the rate determining step represents takes place on going from reactant to the activated complex.The positive value of ΔH° mean that the dissolution reaction is an endothermic process and that dissolution of steel is difficult[18].

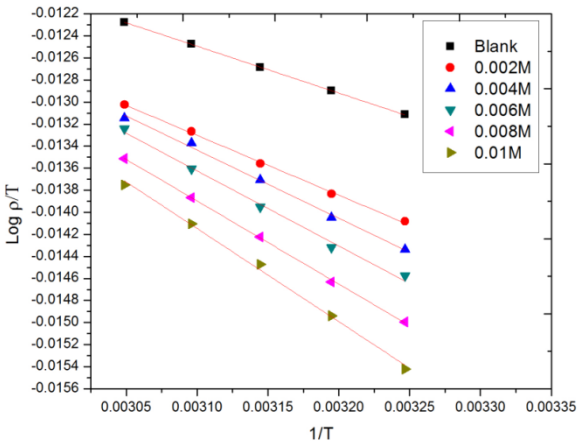

Figure 9: The relation between log ρ/T vs 1/T for mild steel at different concentrations of HMIC.

3.6. SEM Analysis:

The scanning electron microscope images were recorded to establish the interaction of organic molecules with the metal surface. Figure 10 to 11 shows SEM images of polished mild steel surface, mild steel immersed in 2M H_2SO_4 for 24 h, with and without inhibitor.

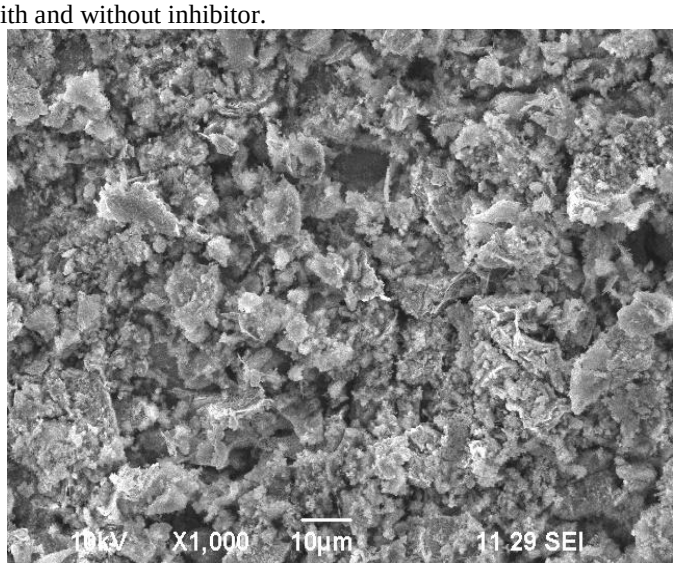

Figure 10: SEM images of mild steel in 2M H_2SO_4 in the absence of inhibitor.

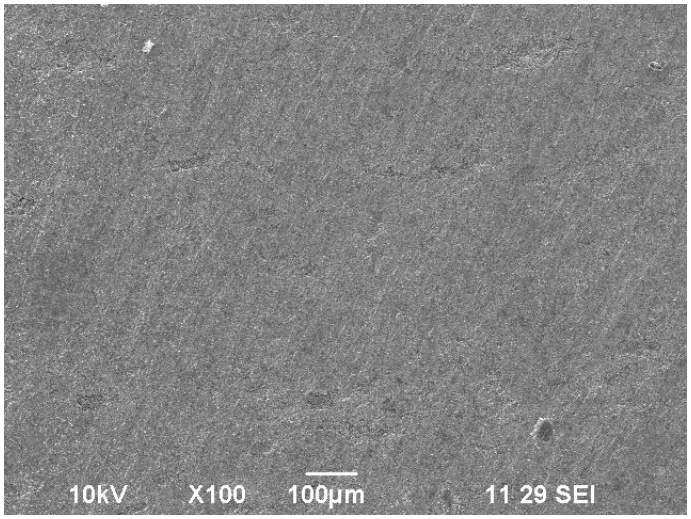

Figure 11: SEM images of mild steel in 2M H_2SO_4 in the presence of inhibitor.

The SEM images revealed that the specimens immersed in the inhibitor solutions are in better conditions having smooth surface, while the metal surface immersed in 2M H_2SO_4 is rough and covered with corrosion products and appeared like full of pits and cavities. This indicated that the inhibitor molecules hindered the dissolution of iron by forming organic film on the steel surface and thereby reduced the rate of corrosion. Hence, the inhibitor protects mild steel in H_2SO_4 solution.

3.7. FT-IR Spectrum:

FT-IR spectral studies were carried out for inhibitor and mild steel surface with inhibitor (Fig. 12) and their respective FT-IR peaks are given in Table 7. In Fig 12(a), $\nu_{(N-H)}$, $\nu_{(C-H)}$, $\nu_{(C=N)}$, $\nu_{(C=C)}$, $\nu_{(C-N)}$ and N-heteroaromatic imidazole ring bands are seen in these compounds, respectively, at 3373.50, 2922.16, 1616.35, 1463.97, 1265.3 and 1379.10cm^{-1}. In Fig 12(b), the IR spectrum of the inhibitor adsorbed on the metal surface reveals the presence of functional group peaks whose absorption frequencies correspond to N-H (shifted from 3373.50 to 3410.15cm^{-1}), C-H (Shifted from 2922.16 to 2941.44cm^{-1}), C=N (shifted from 1616.35 to 1639.49cm^{-1}), C=C (shifted from 1463.97 to 1454.33 cm^{-1}), C-N (shifted from 1265.30 to 1282.66cm^{-1}) and imidazole ring (shifted from 1379.10 to 1361.74cm^{-1}). The shift in the absorption frequencies of the inhibitor on the metal surface supports the interaction between the inhibitor and the metal surface. These changes in the absorption frequencies of IR spectra supported the interaction between functional group of inhibitor with surface of metal [19].

Table 7 Frequencies and assignment of adsorption of FTIR by HMIC and acid containing HMIC

HMIC (frequency in cm^{-1})	**H_2SO_4 containing HMIC (frequency in cm^{-1})**	**Assignment**
3373.50	3410.15	N-H stretch
2922.16	2941.44	C-H stretch
1616.35	1639.49	C=N stretch
1463.97	1454.33	C=C stretch
1379.10	1361.74	N-heteroaromatic imidazole ring
1265.30	1282.66	C-N stretch

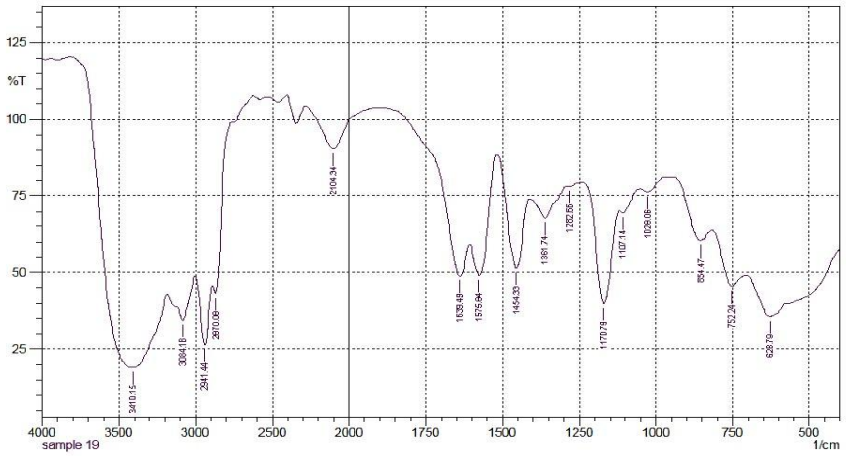

Figure 12 a: FT-IR spectra of HMIC.

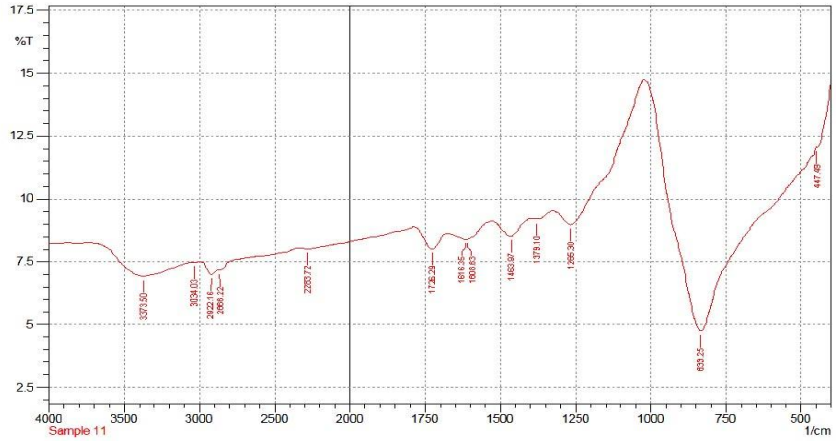

Figure 12b: FT-IR spectra of adsorbed layer formed on the mild steel after immersion in 2M H_2SO_4 containing HMIC.

3.8. Quantum Chemical calculations:

It had been reported that the energy of highest occupied molecular orbital (E_{HOMO}) often associated with the electron donating ability of the molecules. High values of E_{HOMO} indicate a tendency of the molecule to donate electrons to act with acceptor molecules with low-energy, empty molecular orbital. Similarly, the energy of owest unoccupied molecular orbital (E_{LUMO}) represents the ability of the molecule to accept electrons. The lower value of E_{LUMO} suggests the molecule accepts electrons more probable [20]. The calculated quantum chemical indices, E_{HOMO}, E_{LUMO}, energy gap (ΔE) and dipole moment (μ), of investigated compounds are calculated and are shown in Table 8. The results seem to indicate, that charge transfer from the inhibitor takes place during the adsorption to the metal surface. Increasing values of E_{HOMO} and may facilitate adsorption (and therefore inhibition) by influencing the transport process through the adsorbed layer [21]. The dipole moment is another way to obtain data on electronic distribution in a molecule and is one of the properties more used traditionally to discuss and rationalize the structure and reactivity of many chemical systems [22].

Table 8 The calculated quantum chemical parameters for HMIC

Calculated parameters	Values
E_{HOMO} (eV)	-4.7098
E_{LUMO} (eV)	-1.8898
ΔE (E_{HOMO}-E_{LUMO}) (eV)	2.8199
Dipole moment(D)	12.4174

Ionization Potential (eV)	-4.7098
Electron affinity(eV)	-1.8898
ΔN(ev)	1.4100

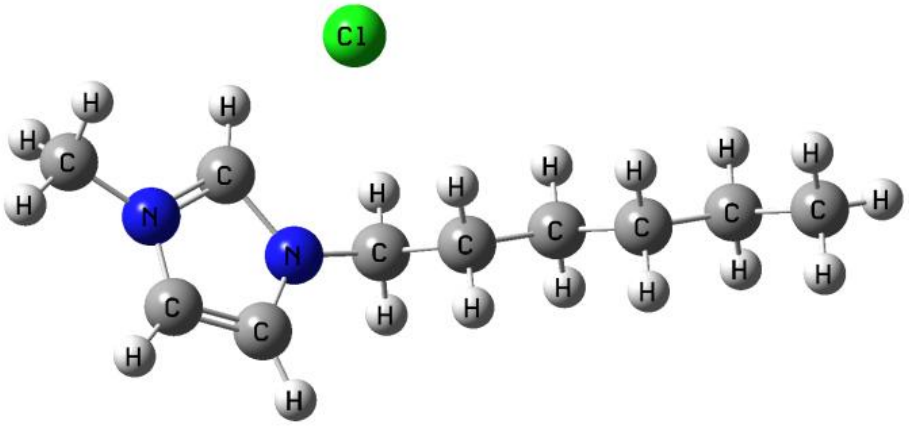

Fig. 13: Optimized molecular structure of HMIC

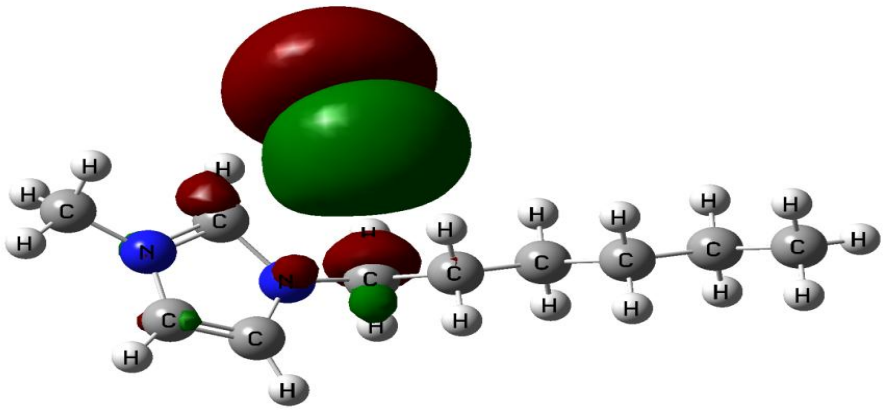

Figure 14a: HOMO surfaces for HMIC molecule.

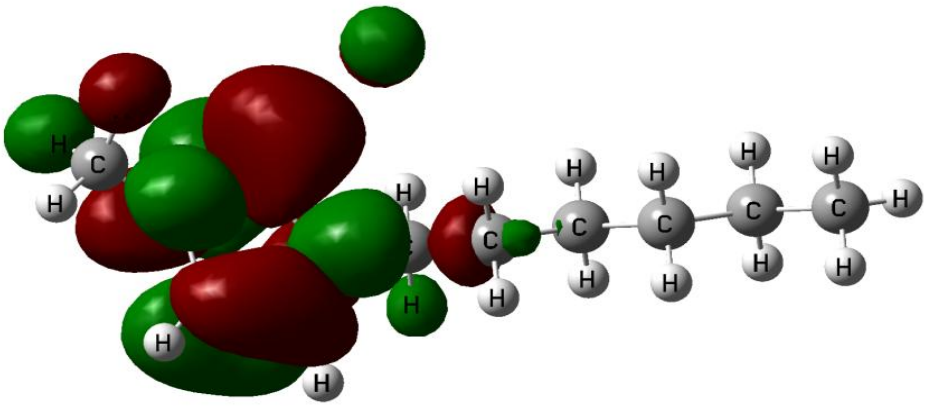

Figure 14b: LUMO surfaces for HMIC molecule.

IV. CONCLUSION

The following are the conclusions drawn from this study:

1. The inhibition efficiency increases and the corrosion rate decreases with increase in HMIC concentration.
2. The inhibition efficiency decreases with increasing the temperatures.
3. Langmuir and Freunlich adsorption isotherms provide an evidence for physisorption.
4. From the polarization studies, it is evident that HMIC act as a mixed type inhibitor.
5. Impedance measurements revealed the increase of charge transfer resistance and decrease of double layer capacitance with increase in the concentration of inhibitor.
6. SEM image was taken for blank acid corroded plate and inhibitor plate. The surface of blank plate has crevices but the inhibitor surface was smooth.
7. FT-IR techniques revealed that a protective film formation on the mild steel surface.
8. The theoretical findings reveal that the differences of inhibiting molecule efficiencies can be explained in terms of the value of sum of electron charge of nitrogen atoms.

REFERENCES

[1.] Donnely B., Downie T C., Grzeskourak R., A study of inhibiting properties of some derivatives of thiourea., *Corrs. Sci*., 14, 1974, 597.

[2.] AbdEiRehim A., Ibrahim M A M., and Khalid K F., The inhibition of 4-(2'-amino-5'-methylphenylazo) antipyrine oncorrosion of mild steel in HCl solution, *Mater. Chem Phys*., 70, 2001, 268-273.

[3.] Lebrini M., Bentiss F., Vezin H., and Lagrenee M., Anti-corrosive properties of S.tinctoria & G. ouregou alkaloid extracts on low carbon steel., *Appl. Surf. Sci*., 25, 2005, 950.

[4.] Ali S A., El-Shareef A M., A1-Ghamdi R F., and Saeed M T., The isoxazolidines: the effect of steric factor and hydrophobic chain length on the corrosion inhibition of mild steel in acidic medium., *Corros. Sci*., 47, 2005, 2659-2678.

[5.] Migahed M A., Electrochemical investigation of the corrosion behavior of mild steel in 2M HCl solution in the presence of 1-dodecyl-4-methoxy pydinium bromide., *Mater.Chem. Phys*., 93, 2005, 48-53.

[6.] Qurashi M A., Khan M A W., Ajmal M., *Anticorros.Methods Mate*r., 43, 1993, 5.

[7.] Andis N Al., Khamis E., Al-Mayouf A., AboulEnicm, H., Electrochemical studies of two corrosion inhibitors for iron in HCl, *Corros. Prev. Control*, 42, 1995, 13.

[8.] Emregul K C., Kurtaran R., Atakol O., Inhibition effect of benzohydrazide derivatives on corrosion behavior of mild steel in 1M HCl., *Corros. Sci*., 45, 2003, 2803.

[9.] Chen S Li., Lei S., Ma H., Yu R., Liu D., Investigation on Schiff bases as HCl corrosion inhibitors for copper.,*Corros. Sci*, 41, 1999, 1273-1287.

[10.] Emregul K C., Atakol O., Corrosion inhibition of mild steel with Schiff base compounds, *Mater. Chem. Phys*, 82, 2003, 188-193.

[11.] E. Bayol, A. A. Gurten, M. Dursun, K. Kayakirilmaz, Adsorption behavior and inhibition corrosion effect of sodium carboxymethyl cellulose on mild steel in acidic medium., Acta Phys. Chim. Sin. 24 (12), 2008, 2236-2242.

[12.] G. Avci., Inhibitor effect of N,N-methylenediacrylamide on corrosion behavior of mild steel in 0.5M HCl., *Mater. Chem. Phys*, 112, 2008, 234-238.

[13.] Umoren S A., Obot I B., Ebenso E E., Obi-Egbedi NO., The inhibition of aluminium corrosion in hydrochloric acid solution by exudates gum from Raphia hookeri., *Desalination*, 247, 2009, 561-572.

[14.] Baharami M J., Hosseini S M A., Pilvar P., Experimental and theoretical investigation of organic compounds as inhibitors., *Corrs.Sci*. 52, 2010, 2793-2803.

[15.] Kalaiselvi P., Chellammal S., Palanichamy S., and Subramanian G., Artemisia pallens as corrosion inhibitor for mild steel in HCl medium.,*Mater. Chem. Phys*., 120, 2010, 643-648.

[16.] Gunavathy N., Murugavel S C., Corrosion Inhibition Studies of Mild Steel in Acid Medium Using Musa Acuminata Fruit Peel Extract., *E- Journal of Chemistry* 9(1), 2012, 487-495.

[17.] Eduok U M., Umoren S A., Udoh A P., *Arabian Journal of Chemistry* (2010), Doi:10.1016/j.arabjc.2010.09.006.

[18.] Guan N M., Xueming L., Fei L., Synergistic inhibition between o-phenanthroline and chloride ion on cold rolled steel corrosion in phosphoric acid.,*Mater. Chem. Phys.* 86, 2004, 59-68.

[19.] Rajappa S K., Venkatesha T V and Praveen B. M.,Chemical treatment of zinc surface and its corrosion studies., *Indian Academy of Sciences*, 2008, 37-41.

[20.] Reisde, F. M.; Melo, H. G.; Costa, EIS investigation on Al 5052 alloy surface preparation for self assembling monolayer., *Electrochim. Acta* 51, 2006, 1780.

[21.] Lukovits, I.; Kalman, E.; Bako, I.; Felhosi, I.; Telegdi, *J. Proc. 8th European Symposium on Corrosion Inhibitors*, Ann. Univ. Ferrara, N.S., Sez V, Suppl. N.10, 1995; p 829.

[22.] Kalil, N. Quantum chemical approach of corrosion inhibition., *Electrochim. Acta* 48, 2003, 2635-2640.